Study of substrata of a slope susceptible to landslide in hilly environment using a geophysical method in The Nilgiris, India

Mathangi Balakrishnan
Vellore Institute of Technology: VIT University
Vladislav Borisovich Zaalishvili
Centre of Russian Academy of Sciences
Ganapathy Pattukandan Ganapathy (seismogans@yahoo.com)
VIT University

Research Article

Keywords: Landslides, MASW, Weak zone, Slip surface, Elastic moduli, Shear moduli

Posted Date: January 12th, 2023

DOI: https://doi.org/10.21203/rs.3.rs-2304020/v1

Abstract

Landslides are one of the prevailing threats to life that causes huge loss to the environment. Around 3.7 million km^2 of the area is exposed to landslides globally and 820,000 km^2 is at high risk for landslides in India. The major triggering factors of landslide in India are rainfall and earthquake. The Nilgiris district which is located in the south-western part of India is more prone to rainfall induced landslides. This study intends to calculate the depth of the slip surface on the slope (Lovedale area, The Nilgiris) in the event of a future landslide using Multichannel Analysis of Surface Waves (MASW). During November 2009 rainfall, a shallow landslide occurred at the toe of this particular slope. Hence, there are more probability for re-occurrence of landslide in the event of rainfall. The shear wave velocity (V_S) obtained from MASW was useful in understanding the variation of the sub-strata and predicting the depth of potential failure surface. The elastic moduli of the soil calculated using empirical relations and software, were compared and one reliable method was considered. The MASW results can be further used for analysing the stability of the slope, reactivation of landslides and landslide early warning system.

1. Introduction

Landslides are one of the natural calamities that cause huge losses to human kind.These can cause both economical and human loss. Generally, rainfall, earthquake, and weak soil are some of the natural triggering factors, whereas cutting the toe of the slope, deforestation, tourism, inadequate drainage, and vibration activities on a weak or steep slope are some of the anthropological factors. In the Indian scenario,the Himalayan and North East mountain terrain in North India, and the Western Ghats from South India contribute to landslides. Landslides in North India are caused due to seismic activities and rainfall whereas Western Ghats undergo 22% of landslides due to rainfall. Rainfall induced landslides can be deadly, unpredictable, and happen very quickly are generally flow and slide type landslide (Highland, L., & Bobrowsky, 2008). Typically, in flow-type landslides, fine soil could result in soil creep or earth flow, while coarse soil could result in debris flow (Varnes, 1978). Landslides are unpredictable and sudden which does not give time to be prepared. So, there is a need to analyse the slope to know whether slope failure will occur or not. Understanding the initiation of a landslide requires a thorough knowledge of the variations in the geology of each slope. Studying the specific behaviour of the sub-structure is required since the type of soil and rock differs with each slope and is typically erratic and complex. To do so, the variability of the soil layers should be delineated, which can be done using Geotechnical and geophysical methods.

Geotechnical methods, which is used in the prediction of slip surface, was formerly achieved through Standard Penetration Test (SPT), Cone Penetration Test (CPT), Pressuremeter, Dilatometer, etc. Even though they provide better results and give a visual picture of the soil sample, they are quite challenging to carry out given the non-plain terrain. Additionally, they provide information about structures beneath the ground only at discrete points, whereas the substructures of mountain terrains are highly undulating. Therefore it is important to find an alternative or a supplement for the geotechnical investigation. One

such method is geophysical investigation which has been in practice since 1921 and has been viewed as a good replacement for geotechnical inquiry (Branagan, 2005). They are non-invasive, take less time, and are simple to carry out on any terrain. This method has become more reliable as a result of the mapping of the underlying soil/rock layer in 1D, 2D, and most recently 3D. This article discusses some of the most popular geophysical techniques that are in use and their feasibility in analysing the slope substructure.

Seismic refraction was one of the earliest geophysical methods employed to measure the depth of bedrock (Jongmans & Garambois, 2007) from 1914 to 1918 during the war. The initial arrival travel time data, which included the direct, refracted and diffracted wave phases, provided the foundation for the seismic refraction approach (Göktürkleret al. 2008). But for shallow depths, a length of the profile of three to five times the necessary depth of penetration was needed. Additionally, waves were attenuated because of very disturbed materials (Jongmans & Garambois, 2007).

Another method that was found was seismic reflection method, that is still in use, was developed in 1921(Dragoset, 2007). High-resolution seismic reflection profiling was a particularly useful tool for imaging the rupture surface, internal bedding, and subsurface geometry of landslide structures (Bruno & Marillier, 2000). But (Jongmans & Garambois, 2007), setting up on uneven terrain was challenging and was time consuming. Additionally, getting the requisite shallow surface soil stratum required a higher signal-to-noise ratio.

Then the Electrical Resistivity Tomography (ERT), a geophysical technique that is often utilised in the hydrogeological investigation of landslides, was developed in 1931 (Slichter, 1933), (Lebourg et al. 2010). This is considered more suitable for landslides occurring at shallow depth (Jongmans & Garambois, 2007). The 2D resistivity images gives a better knowledge of the variation of moisture in the subsurface (Whiteley et al. 2019) (Crawford & Bryson, 2018) (Hen-Jones et al. 2017) (Hibert et al. 2012). However, tomographic inversions were found to be a time-consuming and complicated computational operation (Whiteley et al. 2019) and there is a need for another simple method for shallow-type landslides.

In 1983, a new method was used with only two receivers and one impulsive source called Spectral Analysis of Surface Waves (SASW) to measure the modulii and pavement's thickness (Nazarian et al. 1983). To determine the near-surface shear wave velocity (V_s), this method uses Rayleigh waves into account. It serves a variety of geotechnical and geological functions, but because it was time-consuming to reiterate the same process using only a few receivers across the entire area, an improved version wasdeveloped using multiple receivers using the surface waves. In 1999 Park et al.(1999) developed Multichannel Analysis of Surface Waves (MASW), a more sophisticated version of SASW that uses Rayleigh waves to characterise the subsurface, particularly at shallow depths. Although surface waves were regarded as noise in seismic refraction and reflection methods, here, surface waves with lower frequencies and their dispersive qualities were employed to provide a clear picture of the subsurface at shallow depth (Park et al. 1999) (Park et al. 2007). MASW tests were used extensively on landslide studies by (Xu et al. 2017) (Xu et al.2017) (Mihai et al. 2017) (Suto et al.2016) (Grit & Kanli, 2016) (Lima Júnioret al. 2012) (Su et al. 2017) (Vanl & Senkaya, 2019) (Peng et al. 2017). According to Lima Júnior et

al. (2012), the field configuration is comparable to that of seismic refraction experiments. Lima Júnior et al.(2012) Xu et al. (2017) Mihai et al. (2017) Jongmans et al. (2009) suggested that MASW tests are thought to be more appropriate for shallow landslides and had a higher resolution up to a depth of 20 m (Su et al. 2017) (Xu et al. 2017). The inaccuracy within 5 m depth was only about 10–15% (Berti et al. 2019), and provided better lateral resolution (Harba et al. 2019) making it more dependable.

The geophysical tests performed are correlated with geotechnical properties such as modulus of elasticity, pore water pressure, undisturbed cohesion etc.. Elastic modulii (E and G) which is the slope of the linear part of the stress-strain curve is an important parameter (Fawaz et al. 2014) in geotechnical, transportation engineering, and many other types of infrastructure projects. These require accurate soil characterisation in terms of the Elastic modulus (Sharma et al. 2017). Young's and shear moduli, often known as elastic moduli, describe how stiff a material is in response to elastic deflections (Lu & Kaya, 2014). Many geotechnical investigations such as SPT, CPT, pressuremeter, and dilatometer are used to calculate the modulus of elasticity (Sharma et al. 2017). But as mentioned earlier, these tests are extremely laborious and cost-consuming, especially in hilly terrain. Hence elastic modulus can be obtained from the shear wave velocity (Strelec et al. 2016). Nazarian et al. (1983) conducted SASW for determining the elastic moduli using V_s and V_p (Compression wave velocity) and found that it is in well agreement with cross hole method. But the projected V_P from the MASW study cannot not be taken into account and the shear modulus is considered as only result that we can consider as a reliable approximation of the real value (Moro, 2021). The geophysical tests induces lower shear strain than $3x10^{-4}$% and the shear wave velocity obtained from seismic geophysical tests is appropriate to calculate the shear modulus (G_{max}) (Steven 1996). Hence, the elastic moduli were calculated using V_p and another using density (ρ), poisson's ratio (υ). From this one reliable method was considered to calculate the elastic moduli of the soil which could be used for obtaining the dynamic properties of soil.

This study focuses on analysing variations in the subsoil profile and in determining the depth of a potential failure surface for our study region using MASW. The near-surface stiffness characteristics of the soil components were then correlated with the shear wave velocity that MASW providedusing V_p and another using ρ and υ. The 2D image obtained from MASW will aid in predicting the reactivation of landslide well in advance and may also serve as preliminary data for creating an early warning system.

2. Study Area

Landslides in India are very common in especially in Himalayas and North Eastern mountain range in North India and Western Ghats in South India. Here the area of interest, Western Ghats mountain range, stretches for 1600km, extending its parts at Tami Nadu, Kerala, Karnataka, Maharashtra and Gujarat. In this whole chain, The Nilgiris is more prone to landslides, which is in the West part of Tamil Nadu State (Vulnerability Atlas of India: Background, 2019) as shown in Fig. 1. Flow and slide type landslides are more common in the Western Ghats which can occur at a very high velocity (1m/10 years). The elevation varies from 1000m to 2633m and slope varies in this district from 16 to 30° (Thennavan et al. 2020).

The district is made up primarily of the Peninsular Gneiss Complex-1, Charnokite Gneiss Complex, Laterite/Bauxite, Migamitite Gneiss Complex, and Sathyamangalam Gp. The underlying soil is often silt and clay with a humus zone in the top 0.5 to 1m. The soil layer, which can be found up to 45m beneath the surface, is formed through weathering. The bedrock is composed of Charnokite, a high-grade metamorphic rock that contains garnet, hornblende, hypersthenes, quartz, and feldspar (Seshagiri et al. 1982). The study was conducted in the part of Lovedale which is at south eastern side of The Nilgiris district (11°23'43"N, 76°42'56"E). The slope is 413m length, 2277m high above msl, and the angle of the slope varies from 30° to 15°. It is located in the Charnokite Gneiss complex region, as depicted in Fig. 2. It lies in the high to very high landslide hazard susceptibility zone (Thennavan et al. 2016) (Uvaraj & Neelakantan, 2018) (Biswas et al. 2021).

In the Nilgiris, landslides are triggered by intense rainfall conditions that last for a brief period and by deep infiltration of rainwater. The majority of landslides in the Nilgiris are flow-type landslides (Debris and Earth flow) that can occur very rapidly (Seshagiri et al. 1982) (Uvaraj & Neelakantan, 2018). Major landslides happened in the area in 1902, 1978, 1979, 1993, 2001, 2006, and 2009, and there is a long history of them (Ganapathy & Hada, 2012). Particularly noteworthy was the year 2009 because approximately 1100 landslides that occurred as a result of severe rainfall, which resulted in significant loss of life and property (Thennavan et al. 2016). In the same year high-intensity rain induced a landslide in the study area between November 10th and November 15th of 2009 (Fig. 3), which resulted in a debris flow at the toe of the slope and the destruction of houses as shown in the Fig. 1.Studies on rainfall induced landslide in western Ghats was carried out by (G.P. Ganapathy et al. 2022, G.P. Ganapathy et al. 2021, K. O Chotchaev et al. 2021, R. Gobinath et al, 2021, Gobinath R et al. 2021, G.P. Ganapathy et al 2020, T. Edison et al. 2020, V. B. Svalova et al. 2020, G. Shiyamalagowri et al. 2020, T. Edison and G.P. Ganapathy 2020, V. Senthilkumar et al. 2017). Since the slope of Lovedale has undergone landslide in the past, there are chances of reactivation of the same. The instability that occurred in 2009 was at the toe of the slope, which has a gentle angle of 15°. There are possibilities of re-occurrence of landslide in future, not just at the toe but along the whole slope. Hence it is of prime importance to understand the variation of the geology of the subsurfaceto be prepared in the future event of landslide using MASW.

3. Methodology

Multi Channel Analysis of Surfaace Waves (MASW) was used in the study to investigate the geology and the presence of collapse zone on a slope which is at risk for landslide. It is a non-destructive, cost-effective test, that intends to provide the V_s profile using surface waves with following steps a) Acquisition of ground data, b) Obtaining phase velocity and frequency plot called dispersion curve c) Inversion of dispersion curve to obtain the final shear wave velocity(Park et al. 1999).

3.1. Acquisition of ground data

Shear Wave velocity vary with the wavelength and frequency of the dispersive waves (Xu et al. 2017) and can be obtained using active and passive methods. Bulldozers, electromagnetic shakers, sledgehammers,

weight drops, and other artificially produced vibrations can be utilised as active sources, while nearby vibrating machinery, road-noise, ocean waves, and other noise and vibration can be employed as passive sources (Deyet al. 2012). For the study, active method was used with an impact created using an 8 kg sledge hammer as the seismic source. Geophones are used to receive the seismic source generated from the impact. When comparing geophones of various frequencies, Lima Júnioret al. (2012) determined that 4.5 Hz was preferable since it provided the maximum energy at a lower frequency, leading to a deeper investigation depth (Berti et al. 2019). Depending on the depth of interest, the distance between the geophones may range from 1m to 4m (Foti et al. 2018). The wavelength of the seismic waves affects the depth of the examination as well. More impact from the source will result in a longer wavelength and deeper penetration (Deyet al. 2012). However, it differs from case to instance because it mostly depends on the substratum's velocity structure (Foti et al. 2018). For this reason, 24 nos of vertical geophones of 4.5Hz frequency were used as receivers.

3.2. Dispersion analysis

After data acquisition, an offset- time graph was plotted from the raw data, following that dispersion curves were generated in the phase velocity and frequency domain after removing the noise and applying a low pass filter for frequency in winMASW software. The different range of frequencies were picked from the curve, such as fundamental mode and first higher mode, second higher mode and so on for providing better resolution for deeper depths.

3.3. Inversion analysis

Inversion procedure was carried out utilising genetic algorithm, which is far more accurate than traditional linear inversion (Moro, 2021) to acquire V_s for desired thickness. The equivalent shear wave velocity (V_{sE} or $V_{s,30}$), which is time-averaged for the top 30m is given by

$$V_{s,30} = \frac{\sum_1^N h_i}{\sum_1^N \frac{h_i}{V_{si}}}$$

Where, h_i, is the depth, V_{si} is the shear wave velocity of layer i.

MASW was considered more appropriate for the study area because it offers a dependable V_s profile at shallow depths (Su et al. 2017). Figure 4 and Fig. 5 depicts a schematic representation of MASW operations carried out and field investigation carried out in study area respectively.

The geophone spacing was taken into consideration to be 2m for the profile at the top of the hill (AA') and 2.5m for the profile at the middle of the hill (BB') (shown in Fig. 6). Based on available length, multiple survey points were taken into consideration for each profile. This was done in order to combat the near-field effects, which are undesirable distortions of phase velocity at low frequencies (Foti et al. 2018). A trigger cable, laptop connected to the PASI GEA24 seismograph, 24 vertical geophones, an 8 kg sledge hammer used as the seismic source, and an aluminium plate used as the source impact were the tools utilised (PASI, 2014).

4. Results And Discussions

To determine the depth of a probable failure surface, an in-depth insight into different substrata is needed. This was accomplished by using the shear wave velocity (V_S) measured along the profiles AA' and BB' using MASW as shown in Fig. 6. The receiver spacing used for the investigation were 2m and 2.5m for profile AA’ and BB’ respectively (Table 1). For these profiles, the anticipated depth of investigation was 23 m and 28 m, respectively which were decided depending on the spacing between the geophones. Based on the specifications proposed by (Foti et al. 2018), the depth of interest equals half of the maximum wavelength, this decision was made. The parameters considered for the investigation is summarised in Table 1. The 1D and 2D V_S profile obtained which is an indication of the variation of different soil stratum thickness and type of soil. The average shear wave velocity for top 30m can be calculated using Eq. 1. The results acquired are discussed in the following paragraphs.

Once the raw data were collected from the field, they were analysed with the help of software. To get more accurate subsurface profile at greater depths, the normalised seismic traces, also known as Wiggle plots, of multiple frequency bands were filtered to 25Hz as shown in Fig. 7a.

After muting the noise and filtering the frequency of required range, a 2D f-k spectrum was used to construct the dispersion curve from the wiggle plot, with various modes being chosen at various frequencies Fig. 7b. As shown in Figs. 8a and b, the inversion technique was used to acquire the final one-dimensional (1D) shear wave velocity profile. According to the National Earthquake Hazard Reduction Program's (NEHRP 2020) classification, as shown in Table.2, the soil layers were grouped.

According to Fig. 8a the soil structure for profile AA' increased with increase in depth (1D), from a soft to a very dense state. The shallow layer was 5m thick and had a low-velocity range of 140 to 200 m/s indicating it to be loose unconsolidated granular soil. It was confirmed from the well log report obtained adjacent to the study area (Table 3). Below a layer of 10m (500 m/s), a second weak zone (390–450 m/s) was seen with a thickness of 3m with less weathered charnockite. At a depth of 15m, a high-velocity zone (470 m/s) of partially weathered charnockite was seen.

The superficial layer of profile BB’was thoroughly compacted for agriculture purposes, hence the top soil was denser than the soil at 1 m depth. As a result, the degree of compaction was lower at 1 m depth than it was in the top layer. The shallow layer, included loose sand that is more susceptible to debris flows. The presence of another collapse zone was seen from a depth of 10m indicated by the decrease in velocity from 550 m/s to 490 m/s. This was for a thickness of 10 m indicating the presence of charnockite with more degree of weathering below the less weathered charnockite. At a depth of 23m, a layer of partially weathered rock with a thickness of 6 to 20m was visible. It is to be noted that the 1D V_S shown in Fig. 8a and b are results of only one source point and are discrete. This does not provide any knowledge on the surface of failure and spatial variability of the sub-structure. Hence 2 Dimensional (2D) image was obtained along the depth and the profile length by merging all the 1D profiles which was attained at multiple survey points.

In 2D profile for AA' (as shown in Fig. 9), on the left side of the profile, the V_s range from 140 to 250 m/s for topsoil at a depth of 0–5 m. Due to the presence of loose silty sand, this could be regarded as one of the surfaces that is likely to slip. Due to the presence of a more weathered charnockite layer (300–400 m/s) beneath a thin, weathered charnockite layer (450–500 m/s), another slip surface was found at a depth between 6.5 to 10m. This is so that, although the confining pressure should increase as depth increases, the presence of relatively less dense soil indicates the presence of a weak layer. A continuous charnockite strata (600–760 m/s) was seen 20m below the ground level which agrees well with the lithological data obtained from Public Works Department (PWD).

For the profile BB' potential slip surface, (as shown in Fig. 10), was found at a shallow depth of 0 to 5m and with a velocity of 160 to 360m/s. On the left side of the profile, at a depth of 10m and for a width of 10m, a small pocket of partially weathered charnockite layer was seen. Because soft rocks are prone to fracturing, this layer has a thixotropic effect, particularly at the shallow layer, which may be dangerous. Additionally, a weak zone (500m/s) was discovered beneath the soft rock layer at a depth of 15m and a thickness of 5m.

The consolidated results from MASW was then compared with well log data (Table.3) that was performed adjacent to the study area, correlated well. This is an indication that MASW is one of the geophysical methods that provides better understanding of the geologic structure at shallow depth. It is to be noted that the depth of slip surface was not obtained in the well log data as it is a crude value. Even though MASW tests are easy to perform, non time-consuming and provides consistent results, the V_s obtained can be generally classified. This necessitates a supplement geophysical or geotechnical investigation for an accurate information on sub surface classification.

For further analysis on stability of the slope, the V_s obtained from MASW was used to calculate the elastic moduli of soil using V_s and V_p (Nazarian et al.1983)(Moro, 2021) as given below in Eqs. (2) and (3),

$$G_s = \rho {V_s}^2$$

$$E_s = \rho {V_s}^2 (4 - 3k^2)/(1 - k^2)$$

Where,

G_s is the Shear modulus obtained from the software (MPa)

E_s is the Young's Modulus obtained from the software (Mpa)

ρ is the density of the soil or rock layer at that particular thickness (kg/m^3)

k = V_p/V_s (Dimensionless)

V_p is the Compression wave Velocity (m/s)

V_s is the shear wave velocity (m/s)

The results of elastic moduli calculated from the software were compared with the empirical relations provided by (Stevens, 1996) (Strelec et al. 2016) in Eq. (4), (5), (6),

$$G_e = \rho V_s^2$$

$$\rho = 0.85\log(V_s) - 0.16logh$$

$$E_e = 2G_0(1+\nu)$$

G_e is the Shear modulus calculated from the empirical relations (MPa)

E_e is the Young's modulus calculated from the empirical relations (MPa)

υ is the poisson's ratio

h is the depth (m)

The Variation of elastic modulii (E_e, E_s, G_e and G_s) using two different formulae with respect to depth as contour image using MATLAB is shown in as Fig. 11. The distinctive variation of elastic modulii over profile AA' is shown in Fig. 11a to d, while Fig. 11e to f shows the variation on profile BB'. The E_e and E_s both follow the same pattern over the depth It should also be noted that both the values are fluctuating (i.e neither the E_e is constantly higher nor is the E_s). But predominantly E_e is higher with maximum variation of 20.94% over profile AA' at a depth of 13.4m (Fig. 11a to d). Similarly for the profile BB', the variation between these two values is not considerable but not similar either. It has to be noted that maximum variation was noted at the surficial layer (0 to 0.3m) because compressional velocity V_p, (Uyanik, 2010), increases over porous medium filled with water, while V_s decreases, resulting in an increase in V_p/ V_s. In addition to this, it should be noted that the V_p taken from software is an approximation as mentioned in the manual (Moro, 2021). Hence, it is better to not consider the E_s as a reliable value for analysing the deformation properties of the soil.

Considering the shear modulus, both the values were similar as shown in Fig. 11, since the same parameters were considered in both the equations ρ and υ. But, there was a small variation, because of the considered density of the soil (ρ). The density considered in the empirical formulae depends on V_s and the depth of the layer of interest, whereas it is approximately obtained from the software. Even though there is disparity between these two values, the percentage of variation was very less (as shown in Fig. 11c,11d,11g, 11h), which does not affect the accurate calculation of dynamic propertie of the soil. Hence it is safe to consider both the results as reliable for the dynamic characterization of soil (Stevens, 1996) and V_s is given the prime importance.

5. Conclusions

Landslides in The Nilgiris are the major hazard that causes damage to the human life and to the environment. The goal of the present study was to investigate the slope of Lovedale area that failed in 2009 rainfall, using MASW in order to delineate the sub-soil structure,and to know the depth of the potential slip surface in the event of future landslide. To facilitate this, two MASW tests were conductedalong profile AA’ and BB’, at different parts of the slope, to understand the variation of the depth of slip surface along the longitudinal axis of slope. From the MASW tests conducted on the study area, following conclusions were drawn,

- One Dimensional shear wave velocity profile obtained with respect to depth, aided in knowing the soil stratum at different isolated points. The depth of slip surface (two dimensional profiles) was obtained by interpolating the multiple 1D V_s profile along the profile length.
- Two potential failure surfaces were observed along profile AA', one between 0 to 5m and another between 6.5 to 10m, whereas for profile BB', a slip surface was observed between 0 to 10m, and another between 15m and 20m.
- The results obtained showed that the subterranean strata were properly captured by the geophysical investigation using MASW carried out in the study area. The well log data was used to validate the MASW results, agreed well with each other. But, this log data is crude and discrete which did not provide an idea about the presence of weak zone/surface. Also, when MASW test alone is conducted, there is always a necessity for additional geophysical or geotechnical investigation.
- The elastic moduli (E and G) which is one of the important parameters for calculating dynamic properties of soil, was computed from software which considered V_p and empirical relations that considered ρ and υ. It was noted that Young’s modulus varied at a considerable rate at the surficial layer than at shallow and deeper depths. The reason was attributed to the presence of pores filled with fluid, which increased the V_p/ V_s ratio. The shear Modulus calculated from both software and empirical relations was similar. Even the small differences between the values were because of the variation in the density of the soil. Hence, the shear modulus was considered to be appropriate from both the calculations.
- The integration of MASW and well log data was useful in defining the slope geological structure and identification of depth of the weak zone. The study can be used for further analysis on slope instability modeling, and reactivation of landslides. It can also be considered as a primary information for developing an early warning system for shallow landslides.

Declarations

Ethical Approval

Not applicable

Consent to Participate

All authors agreed to participate in the study

Consent to Publish

All authors read and approved final manuscript

Authors Contributions

All authors contributed to study conception. The field visit and investigation, MASW analysis and first draft of paper writing was done by Mathangi Balakrishnan. Field visit and investigation, paper writing and proof reading was performed by Ganapathy Pattukandan Ganapathy. Part of technical writing and proof reading was done by Vladislav Borisovich Zaalishvili

Corresponding author:

Correspondance to Ganapathy Pattukandan Ganapathy.

Funding

This work was supported by Department of Science and Technology (DST- RFBR Division), Government of India, New Delhi, through the project titled “Natural Hazards and Monitoring of Mountain Territories in Russia and India” (project sanction order DST/INT/RUS/RSF/P-32 dated: 06/09/2019).

Competing Interests

The authors declare no competing interests.

Availability of data and materials

Not applicable

References

1. Berti Matteo, Lara Bertello, and Gabriela Squarzoni. 2019. “Surface-Wave Velocity Measurements of Shear Stiffness of Moving Earthflows.” Landslides 16(3): 469–84.
2. BrototiBiswas, Vignesh K.S, and Rajeev Ranjan. 2021. “Landslide Susceptibility Mapping Using Integrated Approach of Multi-Criteria and Geospatial Techniques at Nilgiris District of India.” Arabian Journal of Geosciences 14(11).
3. Branagan, D. F. 2005. “Historyof Geology From 1900 to 1962.” Encyclopedia of Geology: 185–96.
4. Bruno F., and Marillier. F 2000. “Test of High-Resolution Seismic Reflection and Other Geophysical Techniques on the Boup Lanslide in the Swiss Alps.” Surveys in Geophysics 21(4): 333–48.
5. Chotchaev K. O, Melkov D.A, Ganapathy G.P. (2021), Active dynamics of technogenic landslide on the left board of the Khanikomdon river (North Ossetia), Sustainable Development of Mountain Territories, Vol:13, Issue: 1, pp 66-76, DOI: 10.21177/1998-4502-2021-13-1-66-76

6. Crawford Matthew M., and Sebastian Bryson. L 2018. “Assessment of Active Landslides Using Field Electrical Measurements.” Engineering Geology 233(June 2017): 146–59. https://doi.org/10.1016/j.enggeo.2017.11.012.
7. TaipodiaDey and TaipodiaJumrik, and Arindam Dey. 2012. “A Review of Active and Passive MASW Techniques.” (October 2016).
8. Dragoset Bill. 2007. “A Historical Reflection on Reflections.” Hart’s E and P (DEC.): 46–70.
9. Edison T., Ganapathy G.P, Chandrasekaran S.S. and Rajawat, A.S. (2020), Probabilistic rainfall thresholds for shallow landslides initiation – A case study from The Nilgiris district, Western Ghats, India. International Journal of Disaster Risk Management, 2(1), 1-14. https://doi.org/10.18485/ijdrm.2020.2.1.1.
10. Edison. T. and Ganapathy .G.P. (2020), Evaluation of Landslide Hazard and its Impacts on Hilly Environment of The Nilgiris District - A Geospatial Approach, Geoenvironmental Disasters, Vol 7 (3), pp 1-14. DOI: https://doi.org/10.1186/s40677-019-0139-3
11. Fawaz A, Hagechehade. F and Farah. E 2014. “A Study of the Pressuremeter Modulus and Its Comparison to the Elastic Modulus of Soil.” Study of Civil Engineering and Architecture 3. www.seipub.org/scea.
12. Foti, Sebastiano et al. 2018. 16 Bulletin of Earthquake Engineering Guidelines for the Good Practice of Surface Wave Analysis: A Product of the InterPACIFIC Project.
13. Ganapathy G.P., Srinivasan. K., Datta D.., Chang C.,. Purohit O, Vladislav Zaalishvili, Olga Burdzieva (2022). Rainfall Forecasting Using Machine Learning Algorithms for Localized Events. CMC-Computers, Materials & Continua, 71(3), 6333–6350.
14. Ganapathy G.P., Zaalishvili V.B., Melkov D.A, Kazieva. F. B, (2021)Landslides rainfall thresholds approaches for the Western Ghats India and the North Caucasus (Russia) Sustainable Development of Mountain Territories, Vol:13, Issue: 3, Pg.No(379-386), DOI: 10.21177/1998-4502-2021-13-3-379-386
15. Ganapathy G.P., Zaalishvili V.B., Chandrasekaran S.S., and. Melkov D.A (2020), Integrated Monitoring of Slope Process, in India and Russia, Sustainable Development of Mountain Territories, Vol. No 4 (46), pp. 573-582, DOI: 10.21177/1998-4502-2020- 12-3-349-356.
16. Ganapathy G. P., and Hada. C. L. 2012. “Landslide Hazard Mitigation in the Nilgiris District, India – Environmental and Societal Issues.” International Journal of Environmental Science and Development (March): 497–500.
17. Gobinath R., Ganapathy G.P. , and Akinwumi I.I. (2021), Stabilisation of Natural Slopes using natural plant root as reinforcing agent, Elsevier - Materials Today: Proceedings, Vol. 39, Part 1, pp 493-499 DOI: https://doi.org/10.1016/j.matpr.2020.08.227.
18. Gobinath R., Ganapathy G.P., Akinwumi I.I., Prasath E., Raja G., Prakash T., Shyamala G., (2021), Soil erosion protection on hilly regions using plant roots: An experimental insight, Advances in Science, Technology and Innovation, pp. 321-335, DOI: 10.1007/978-3-030-23243-6_20.

19. Gobinath R., Ganapathy G.P., and Salunke A.A., Prasath E (2020), Understanding Soil Erosion Protection Capabilities of Four Different Plants on Silty Soil, IOP Conf. Series: Materials Science and Engineering, 981 032053, pp 1-8, DOI: doi:10.1088/1757-899X/981/3/032053.
20. Göktürkler Gökhan, Çağlayan Balkaya, and Zülfikar Erhan. 2008. “Geophysical Investigation of a Landslide: The Alt1ndağ Landslide Site, İzmir (Western Turkey).” Journal of Applied Geophysics 65(2): 84–96.
21. Grit Mert, and Ali Ismet Kanli. 2016. “Integrated Seismic Survey for Detecting Landslide Effects on High Speed Rail Line at Istanbul-Turkey.” Open Geosciences 8(1): 161–73.
22. Harba Paulina, Zenon Pilecki, and Krzysztof Krawiec. 2019. “Comparison of MASW and Seismic Interferometry with Use of Ambient Noise for Estimation of S-Wave Velocity Field in Landslide Subsurface.” Acta Geophysica 67(6): 1875–83. https://doi.org/10.1007/s11600-019-00344-9.
23. Hen-Jones, R. M. Hughes, P. N. Stirling, R. A. Glendinning, S. Chambers, J. E. Gunn, D. A. Cui, Y. J. 2017. “Seasonal Effects on Geophysical–Geotechnical Relationships and Their Implications for Electrical Resistivity Tomography Monitoring of Slopes.” Acta Geotechnica 12(5): 1159–73.
24. Hibert, Clément, Grandjean Gilles, Bitri Adnand, Travelletti Julien Malet, and Jean Philippe 2012. “Characterizing Landslides through Geophysical Data Fusion: Example of the La Valette Landslide (France).” Engineering Geology 128: 23–29.
25. Highland, L., & Bobrowsky, P. T. 2008. The Landslide Handbook — A Guide to Understanding Landslides. Reston: US Geological Survey.
26. Jongmans, D. Bièvre, G. Renalier, F. Schwartz, S. Beaurez, N. Orengo, Y.. 2009. “Geophysical Investigation of a Large Landslide in Glaciolacustrine Clays in the Trièves Area (French Alps).” Engineering Geology 109(1–2): 45–56. http://dx.doi.org/10.1016/j.enggeo.2008.10.005.
27. Jongmans, Denis, and Stéphane Garambois. 2007. “Geophysical Investigation of Landslides: A Review.” Bulletin de la Societe Geologique de France 178(2): 101–12.
28. Lebourg, T. Hernandez, M. Zerathe, S. El Bedoui, S Jomard, H. Fresia, B.2010. “Landslides Triggered Factors Analysed by Time Lapse Electrical Survey and Multidimensional Statistical Approach.” Engineering Geology 114(3–4): 238–50. http://dx.doi.org/10.1016/j.enggeo.2010.05.001.
29. Lima Júnior, Sérgio Bezerra, Renato Luiz Prado, and Rodolfo Moreda Mendes. 2012. “Application of Multichannel Analysis of Surface Waves Method (MASW) in an Area Susceptible to Landslide at Ubatuba City, Brazil.” Revista Brasileira de Geofisica 30(2): 213–24.
30. Lu, Ning, and Murat Kaya. 2014. “Power Law for Elastic Moduli of Unsaturated Soil.” Journal of Geotechnical and Geoenvironmental Engineering 140(1): 46–56.
31. Mihai, Marinescu, Cristea Paul, Marunteanu Cristian, and Mezincescu Matei. 2017. “MASW Seismic Method in Brebu Landslide Area, Romania.” IOP Conference Series: Earth and Environmental Science 95(3).
32. Moro, Giancarlo Dal. 2021. “Surface Wave Analysis for near Surface Applications (Manual).” 1–357. www.winmasw.com.

33. Nazarian, Soheil, Kenneth H. Stokoe, and W. R. Hudson. 1983. “Use of Spectral Analysis of Surface Waves Method for Determination of Moduli and Thicknesses of Pavement Systems.” Transportation Research Record: 38–45.
34. NEHRP Recommended Seismic Provisions for New Buildings and Other Structures.2020. BUILDING SEISMIC SAFETY COUNCIL I (September).
35. Park, Choon B., Miller, Richard D., Xia, Jianghai, and Ivanov, Julian. 2007. “The Conventional Seismic.” The Leading Edge.
36. Park, Choon B., Richard D. Miller, and Jianghai Xia. 1999. “Multichannel Analysis of Surface Waves.” Geophysics 64(3): 800–808.
37. PASI. 2014. User Manual Seismograph GEA24 P.A.S.I. www.pasisrl.it.
38. Peng, Jianbing, Gonghui Wang, Qiyao Wang, and Fanyu Zhang. 2017. “Shear Wave Velocity Imaging of Landslide Debris Deposited on an Erodible Bed and Possible Movement Mechanism for a Loess Landslide in Jingyang, Xi’an, China.” Landslides 14(4): 1503–12.
39. Senthilkumar, V., S. S. Chandrasekaran, and V. B. Maji. 2017. “Geotechnical Characterization and Analysis of Rainfall—Induced 2009 Landslide at Marappalam Area of Nilgiris District, Tamil Nadu State, India.” Landslides 14(5): 1803–14.
40. Seshagiri DN, Badrinarayanan S, Upendran R, Lakshmikantham et al (1982) The Nilgiris landslide—miscellaneous publication No. 57. Geological Survey of India.
41. Sharma L. K., Rajesh Singh, R. K. Umrao, K. M. Sharma, T. N. Singh 2017. “Evaluating the Modulus of Elasticity of Soil Using Soft Computing System.” Engineering with Computers 33(3): 497–507.
42. Shiyamalagowri G., Ganapathy. G.P. , Vladislav Zaalishvili, Dmitry Melkov (2020), Partitioning around medoids approach application for computation of regional flood and landslide quantiles, Environmental Engineering, E3S Web of Conferences, Volume 157, 02001 (2020) Key Trends in Transportation Innovation KTTI-*2019.* https://doi.org/10.1051/e3sconf/202015702001.
43. Slichter, L. B. 1933. “The Interpretation of the Resistivity Prospecting Method for Horizontal Structures.” Journal of Applied Physics 4(9): 307–22.
44. Steven Kramer. 1996. Geotechnical Earthquake Engineering. Prentice-Hall, New Jersey.
45. Strelec, Stjepan, Davor Stanko, and Mario Gazdek. 2016. “Empirical Correlation between the Shear-Wave Velocity and the Dynamic Probing Heavy Test: Case Study, Varaždin, Croatia.” Acta Geotechnica Slovenica 13(1): 3–15.
46. Su, Li jun, Xing qian Xu, Xue yu Geng, and Shuang qing Liang. 2017. “An Integrated Geophysical Approach for Investigating Hydro-Geological Characteristics of a Debris Landslide in the Wenchuan Earthquake Area.” Engineering Geology 219: 52–63.
47. Suto, Koya, Milovan Urosevic, and Snezana Komatina. 2016. “An MASW Survey for Landslide Risk Assessment: A Case Study in Valjevo, Serbia.” Chiang Mai Journal of Science 43(Special Issue 2): 1249–58.

48. Svalova V. B., Zaalishvili V. B., Ganapathy G. P., Ivanov P. G. (2020), Engineering and technical methods for landslide risk management and reduction, Scientific Journal Sustainable development of Mountain Territories, Volume .12. №1(43), pp. 162 -170 DOI: 10.21177/1998-4502-2020- 12-1-162-170.
49. Thennavan, Edison, Ganapathy Ganapathy Pattukandan, S S Chandrasekaran, and Ajay S Rajawat. 2020. “Probabilistic Rainfall Thresholds for Shallow Landslides Initiation – A Case Study from the Nilgiris District, Western Ghats, India.” International Journal of Disaster Risk Management 2(1): 1–13.
50. Thennavan, Edison, Ganapathy Pattukandan Ganapathy, Chandra Sekaran. S.S and Ajay S. Rajawat. 2016. “Use of GIS in Assessing Building Vulnerability for Landslide Hazard in The Nilgiris, Western Ghats, India.” Natural Hazards 82(2): 1031–50.
51. Uvaraj, S., and Neelakantan. R 2018. “Fuzzy Logic Approach for Landslide Hazard Zonation Mapping Using GIS: A Case Study of Nilgiris.” Modeling Earth Systems and Environment 4(2): 685–98. http://dx.doi.org/10.1007/s40808-018-0447-8.
52. Uyanik, Osman. 2010. “Compressional and Shear-Wave Velocity Measurements in Unconsolidated Top-Soil and Comparison of the Results.” International Journal of Physical Sciences 5(7): 1034–39.
53. Senthilkumar. V, Chandrasekaran S.S and Maji. V.B 2017. “Overview of Rainfall Induced Landslide Events and Importance of Geotechnical Investigations in Nilgiris District of Tamil Nadu, India.” In Advancing Culture of Living with Landslides, , 281–87.
54. Vanl, Gulseda, and Mustafa Senkaya. 2019. “Integrated Shallow Seismic Imaging of a Settlement Located in a Historical Landslide Area.”
55. Varnes, D. 1978. “Slope Movement Types and Processes.” Special report 176: 11–33.
56. Vulnerability Atlas of India: Background. 2019. 3rd ed. Building Materials and Technology Council. https://www.bmtpc.org/DataFiles/CMS/file/VAI2019/background.pdf.
57. Whiteley, J. S. Chambers, J. E. Uhlemann, S. Wilkinson, P. B. Kendall, J. M.2019. “Geophysical Monitoring of Moisture-Induced Landslides: A Review.” Reviews of Geophysics 57(1): 106–45.
58. Xu, Xing qian, Li jun Su, and Chao Liu. 2016. “The Spatial Distribution Characteristics of Shallow Fissures of a Landslide in the Wenchuan Earthquake Area.” Journal of Mountain Science 13(9): 1544–57.
59. Xu, Xing qian, Li jun Su, Guang da Zhang, and Hong hu Zhu. 2017. “Analysis on Shear Wave Velocity Structure of a Gravel Landslide Based on Dual-Source Surface Wave Method.” Landslides 14(3): 1127–37. http://dx.doi.org/10.1007/s10346-016-0780-9.

Tables

Table.1 NEHRP classification of subsurface based on shear wave velocity (NEHRP 2020)

Site Class	Soil Profile	$V_{s(avg)}$ (m/s)
A	Hard rock	> 1524
B	Medium Hard rock	> 914 to 1524
BC	Soft rock	> 640 to 914
C	Very dense sand or hard clay	> 442 to 640
CD	Dense sand or Very stiff clay	> 305 to 442
D	Medium dense sand or stiff clay	> 213 to 305
DE	Loose sand or medium stiff clay	> 152 to 213
E	Very loose sand or soft clay	< 152
F	Soils requiring site response analysis	-

Table.2 Parameters considered for MASW performed in the study area

Parameters	Parameters suggested by (Foti et al. 2018)	Parameters considered for profile AA'	Parameters considered for profile BB'
Geophone spacing	1-4m	2m	2.5m
Array length	23-96m	53m	62.5m
Number of geophones	24 or 48	24 nos	24 nos
Offset between 1st geophone and source	5-20m	5m	5m
Sampling interval	0.5ms	0.5ms	0.5ms
Post trigger recording length	2s	2s	2s
Pre-trigger recording length	0.1-0.2s	0.1s	0.1s

Table.3 Well log data obtained adjacent to the study area (Source: Public Works Department)

Well No	Depth (m)	Lithology from Well log data	Lithology from MASW	Colour	Texture	Shape
HP2NIL03	0.5	Topsoil	Loose unconsolidated soil	brown	coarse to very coarse	rounded
HP2NIL03	3	Weathered charnockite	Medium Dense Sand/Stiff clay	blackish Blue	medium	Sub angular
HP2NIL03	20	Partially weathered charnockite	Soft rock	blackish Blue	medium	Sub angular

Figures

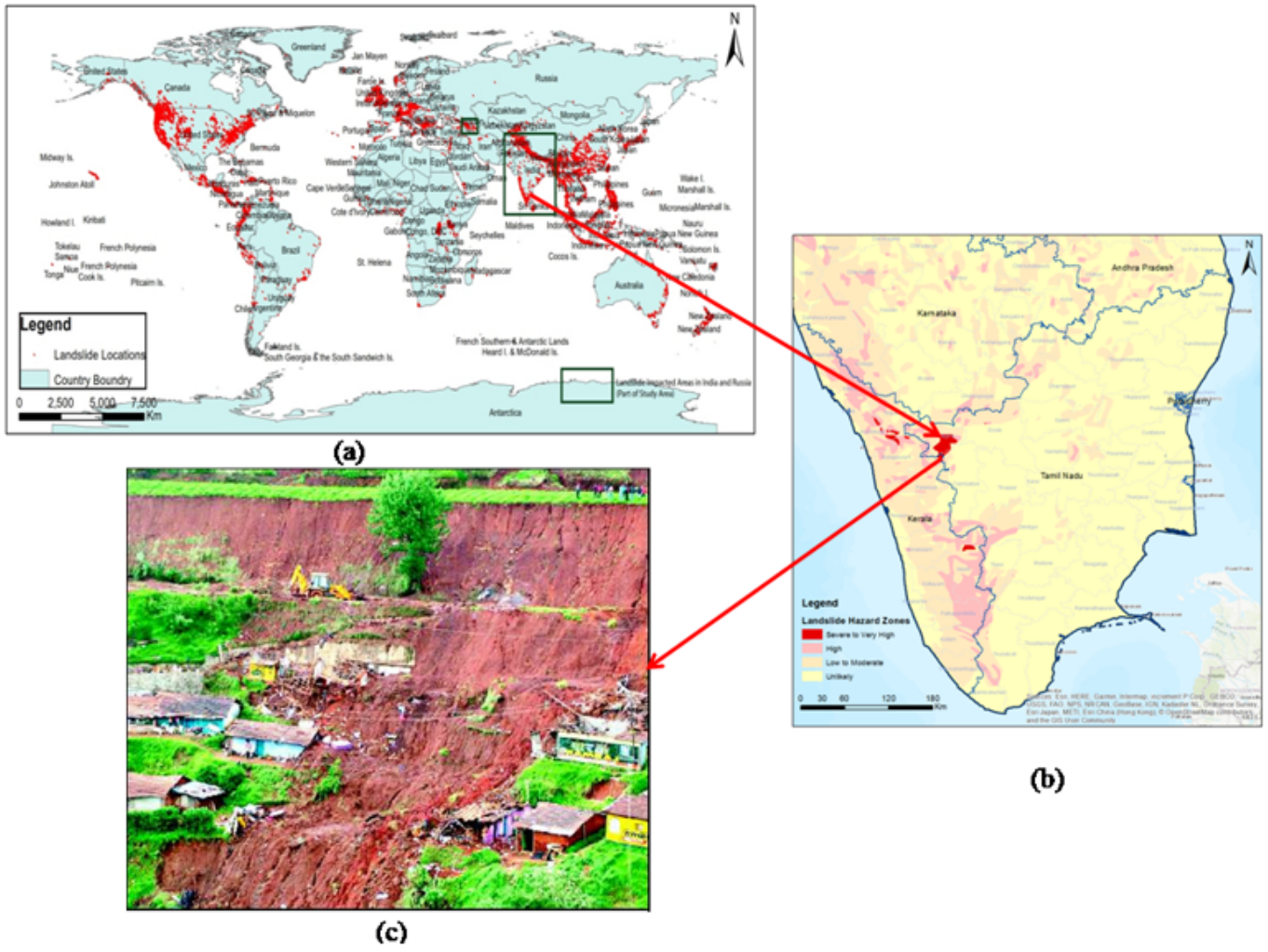

Figure 1

(a) Global landslide inventory map (b) Landslide hazard map of South India (c) Location of Lovedale Landslide occurred in 2009 (Source: dnaindia).

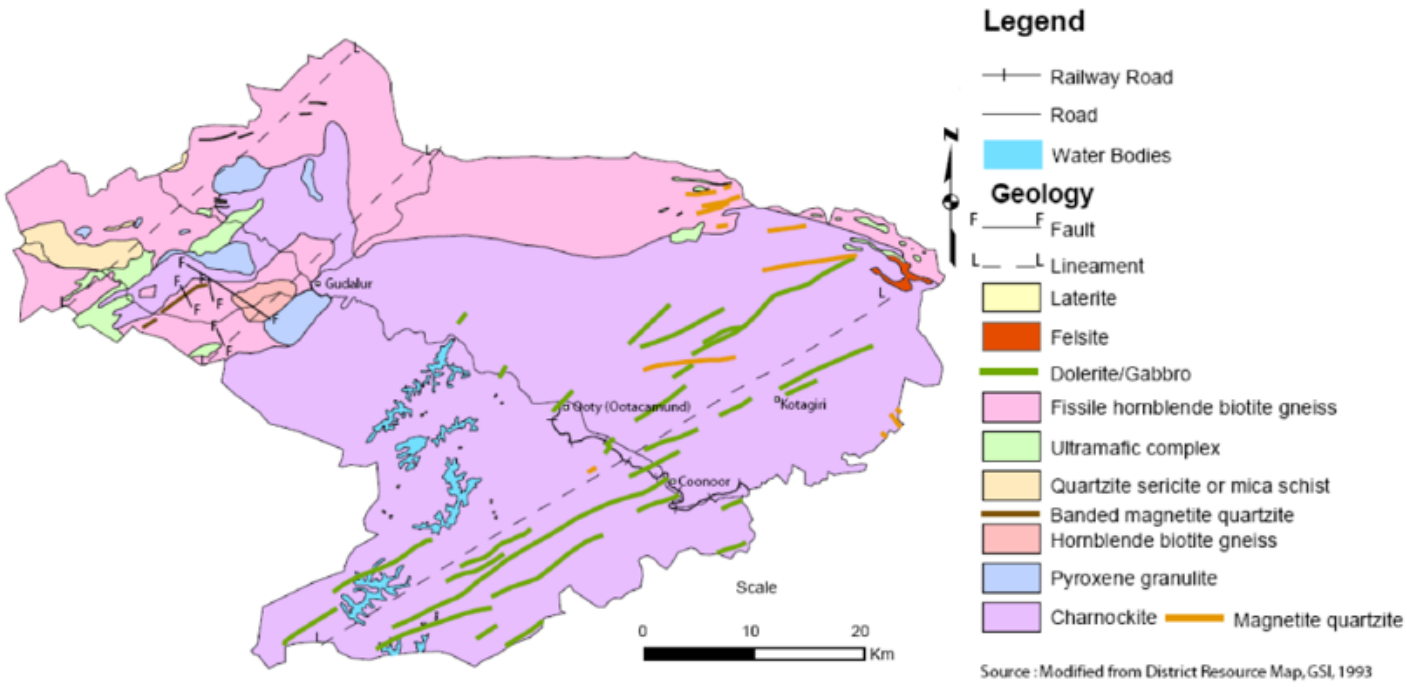

Figure 2

Geological map of the study area

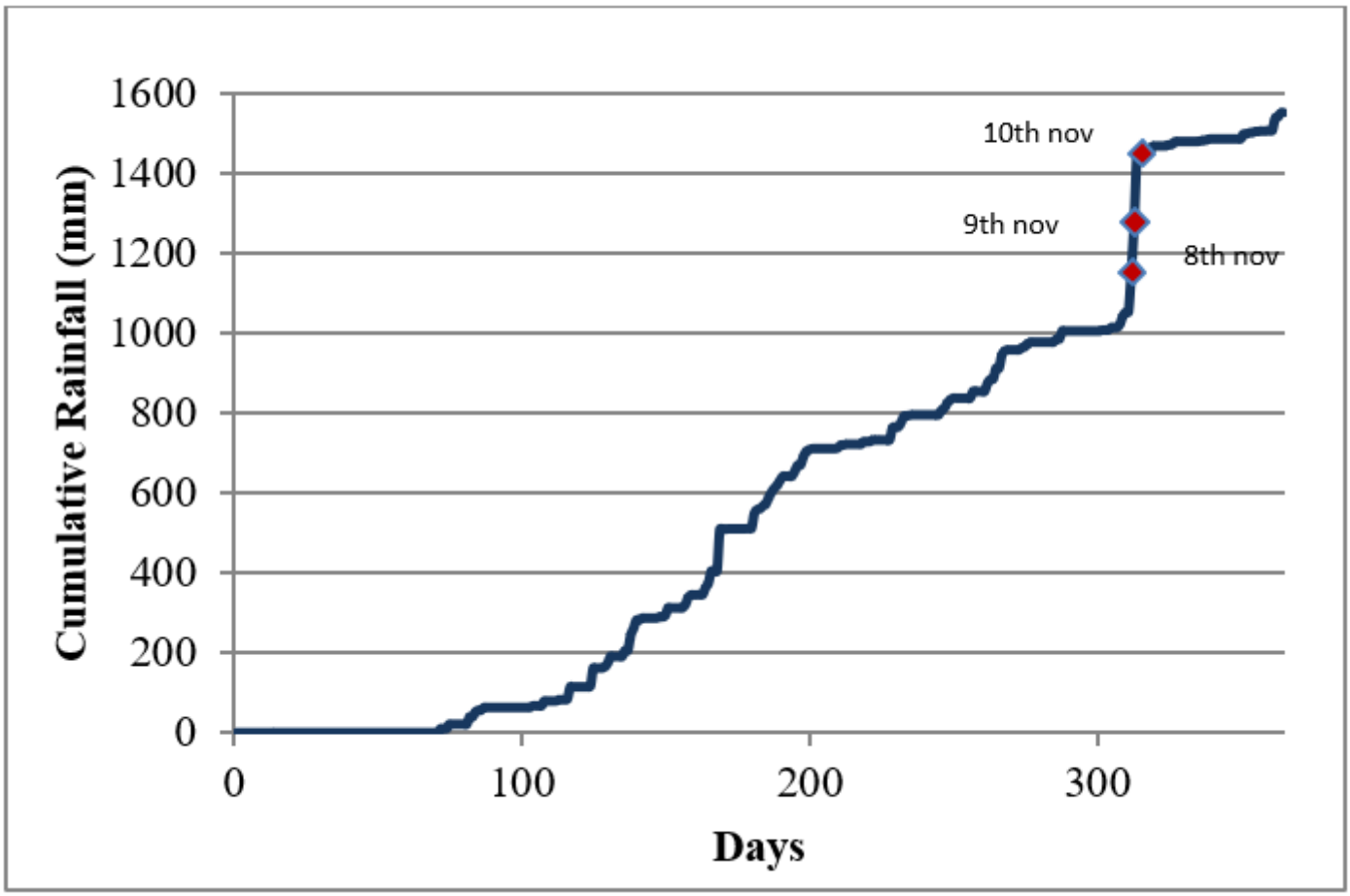

Figure 3

Cumulative rainfall for the year 2009

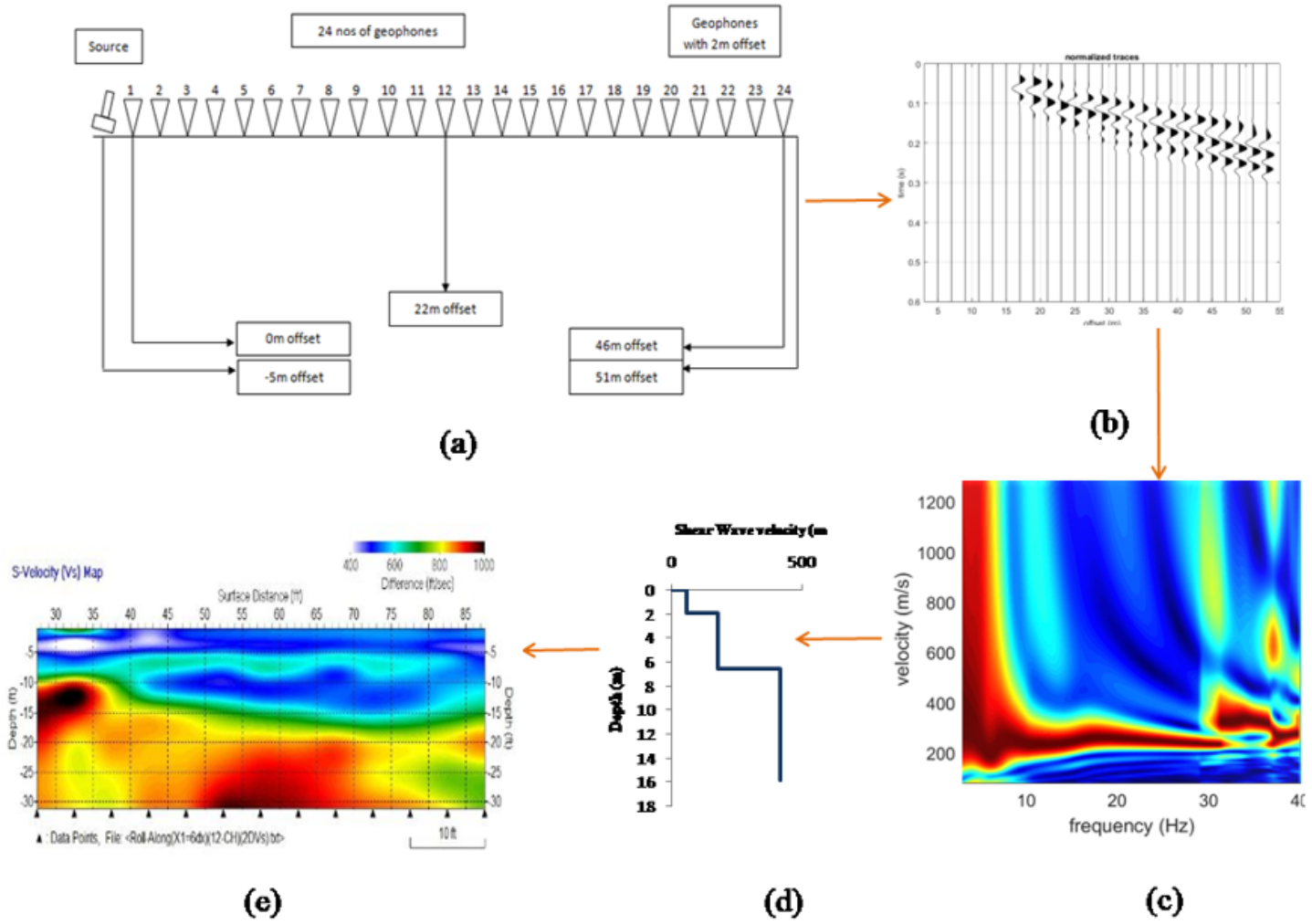

Figure 4

Schematic diagram of MASW setup (a) Field set up (b) Normalised seismic traces (c) Dispersion Curve (d) 1D Shear Wave velocity curve (e) 2D Shear Wave velocity (Source: Park seismic LLC)

Figure 5

MASW test performed at the study area

Figure 6

Section AA' and BB' where MASW tests were performed in the study area (Source: Google earth images)

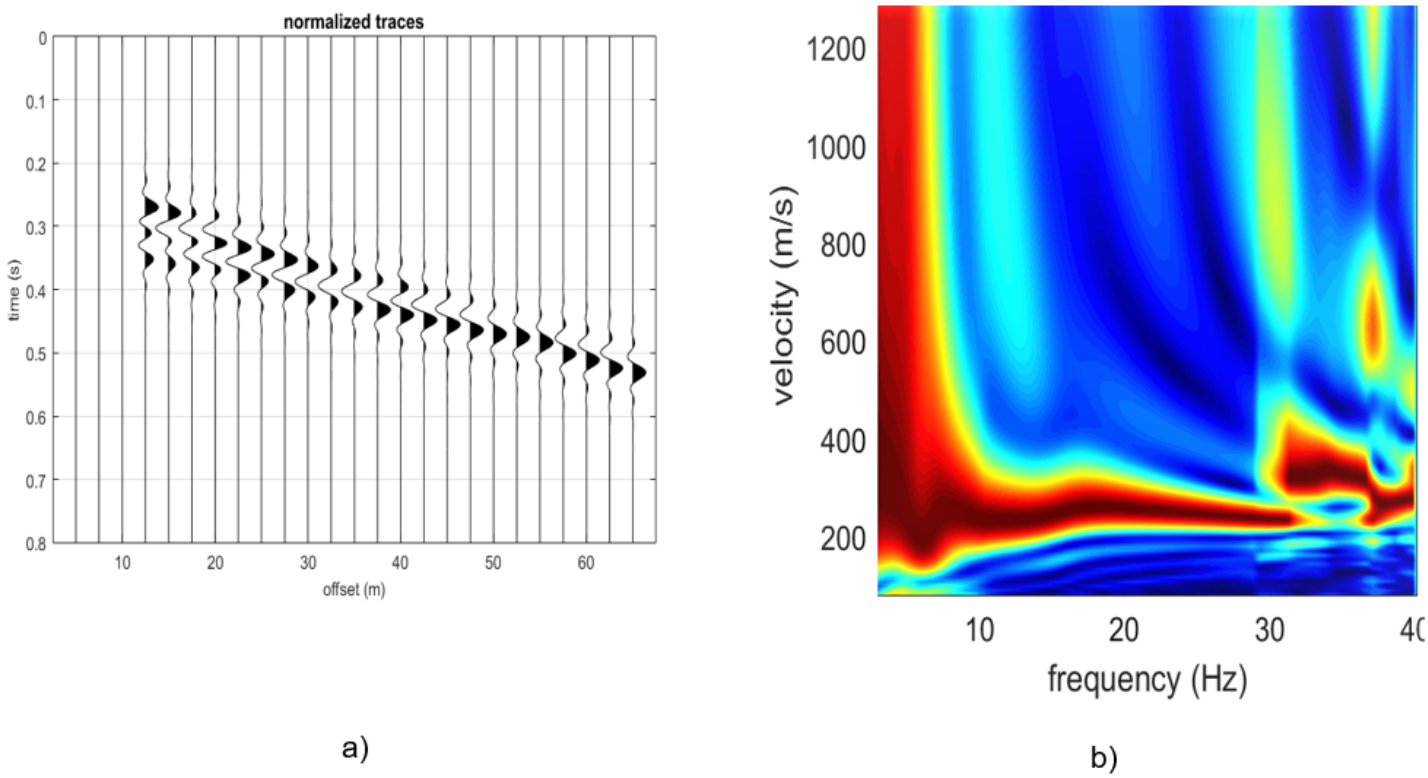

Figure 7

(a)SampleSeismic records obtained from the site in time- offset domain (b) Dispersion curve obtained in frequency- velocity domain

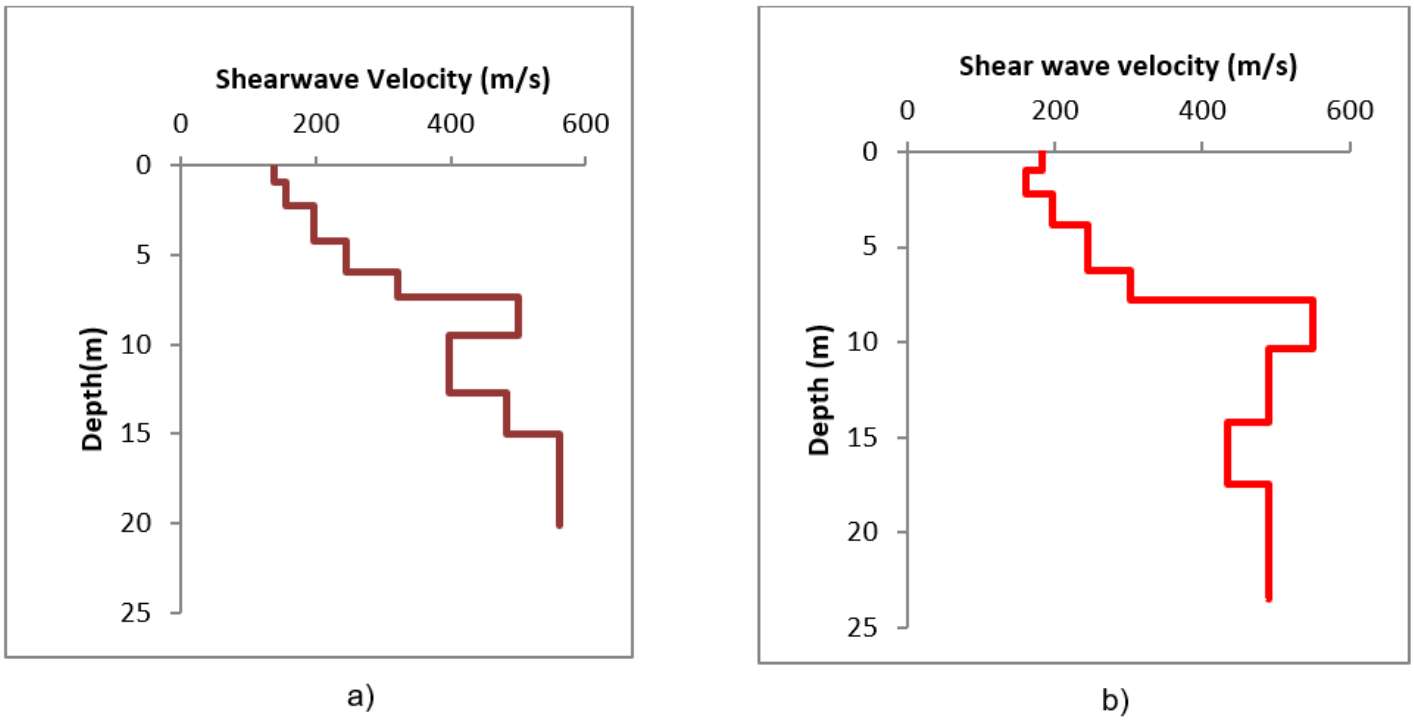

Figure 8

1D shear wave velocity for (a) Profile AA’ (b) Profile BB’

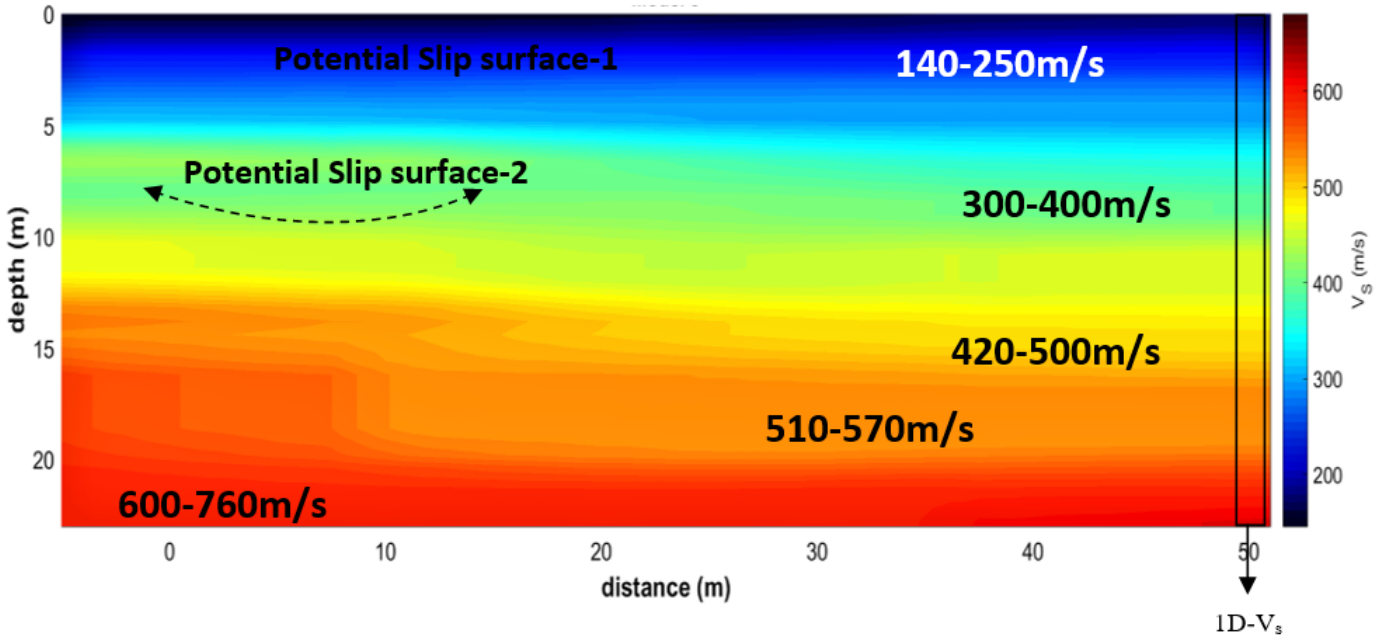

Figure 9

2D shear wave velocity profile obtained for profile AA’

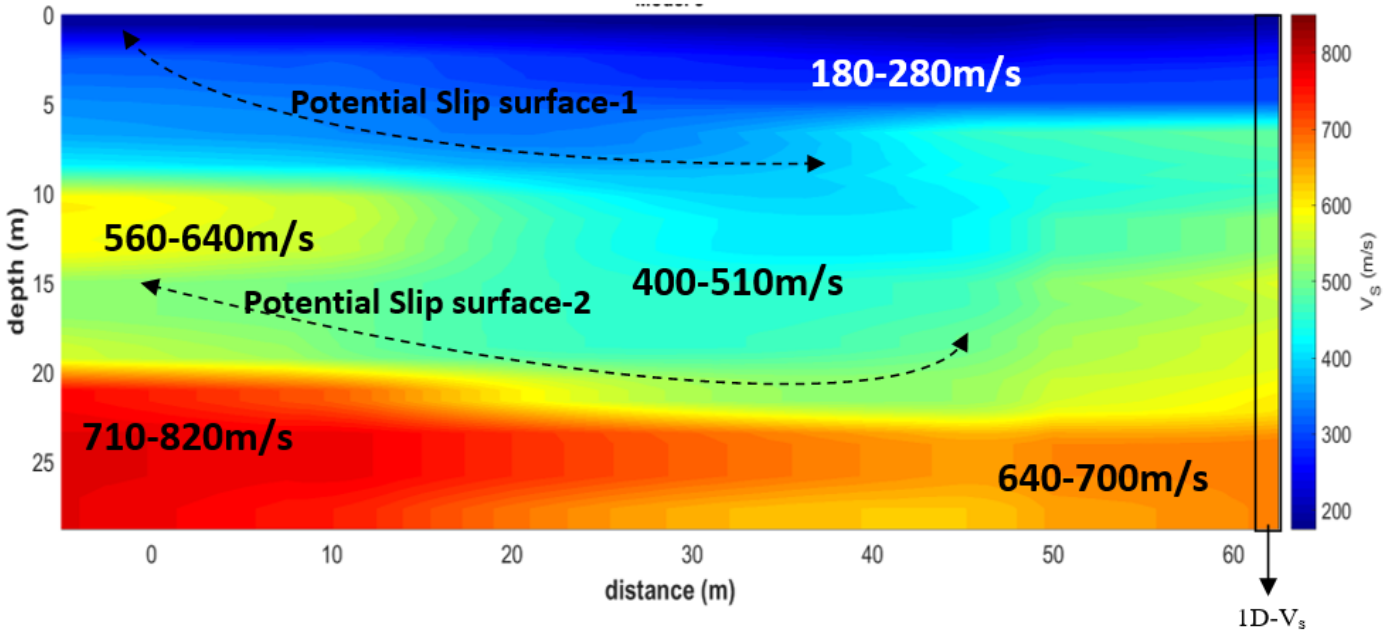

Figure 10

2D shear wave velocity obtained for profile BB’

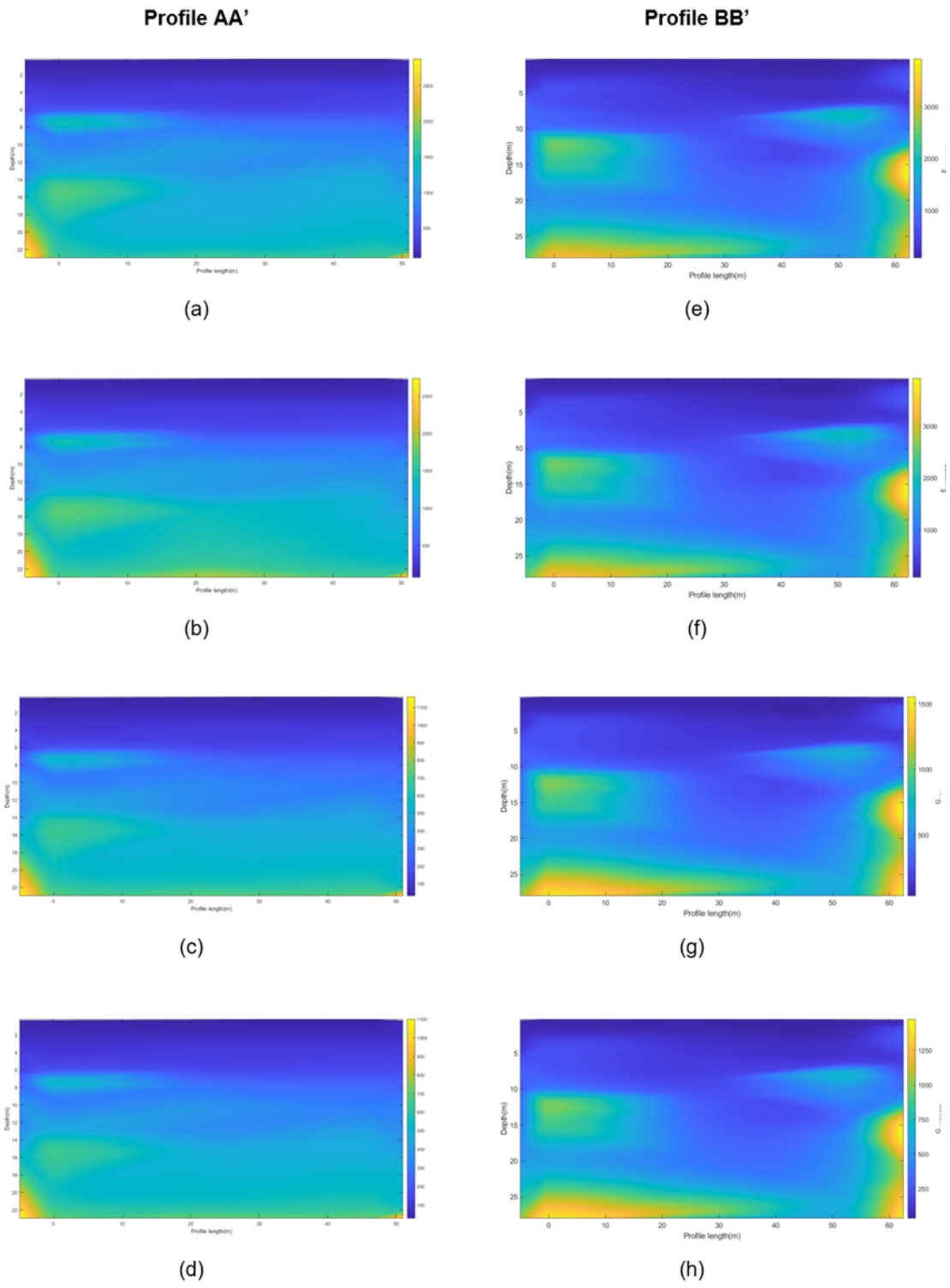

Figure 11

Contour image for profile AA' Young's modulus calculated using (a) Empirical relations (b) Software, Shear modulus calculated using (a) Empirical relation (d) Software and Profile BB' Young's modulus calculated using (e) Empirical relations (f) Software, Shear modulus calculated using (g) Empirical relation (h) Software

Supplementary Files

This is a list of supplementary files associated with this preprint. Click to download.

- Questionsandanswers.pdf